Modeling and Simulation of Biologically Inspired Flow Field Designs for Proton Exchange Membrane Fuel Cells

A. Arvay[a], J. French[a], J.-C. Wang[a], X.-H.Peng[b] and A.M. Kannan[a],*

[a]*Fuel Cell Laboratory, Department of Engineering and Computing Systems, Arizona State University, Mesa, AZ 85212, USA*

[b]*School of Letters and Sciences, Arizona State University, Mesa, AZ 85212, USA*

Abstract: Various biologically inspired flow field designs of the gas distributor (interconnector) have been designed and simulated. Their performance using Nafion-212 with humidified H_2 and Air at 80 ^{o}C with the ANSYS Fluent Fuel Cell module software was evaluated. Novel interdigitated designs were optimized by obeying biologically inspired branching rules. These rules allow for more mathematically formal descriptions of flow field designs, enabling relatively simple optimization. The channel to land ratio was kept equivalent between designs with typical values between 0.8 and 1.0. The pressure drop and the current density distribution were monitored for each design on both anode and cathode sides. The most promising designs are expected to exhibit lower pressure drop however, low pressure drop can also be an indication of potential water flooding at higher operating current density. A biologically inspired interdigitated design with 9 inlet channels exhibited reduced pressure drop and improved current density distribution compared to all other interdigitated designs evaluated in this study. The simulated fuel cell performance data at ambient pressure with humidified H_2 and air compares well with the experimental data using a single serpentine flow field design.

1. INTRODUCTION

Proton exchange membrane fuel cells (PEMFCs) are electrochemical devices that convert hydrogen and oxygen to electricity, heat, and water. PEMFCs generate this energy with no greenhouse gas emission and can operate at temperatures from below freezing to 90 ^{o}C. This makes PEMFCs especially attractive for transportation applications [1]. There are several critical challenges to overcome before PEMFC technology becomes a viable competitor to existing automotive engines. One of the key components is the gas flow field design, which must be optimized to satisfy several conflicting requirements.

The primary role of the flow field is to deliver reactant gasses to the reaction sites. Non-uniform gas delivery will result in different reaction rates at different areas of the cell. Areas of the cell that are starved of reactant gasses will exhibit lower reaction rates which reduce the over all efficiency of the cell. At the other end of the spectrum, areas of higher reaction rates can create local hot spots due to heat from the reaction and ohmic heating. These high temperature areas may damage the membrane and reduce the perfor-mance and life of the cell.

The flow field must also be designed to maintain proper water balance within the cell. The Nafion membrane in a PEMFC requires moisture in order to maintain proton conductivity. But it is essential that excess water formed during the chemical reaction be transported away from reaction sites in order to maintain high performance. Flooding is especially problematic at high current densities when there is a large amount of product water generation. Many parallel designs retain water which can make them more appropriate at low power draw, however at high power draw they have a tendency to flood which reduces performance. Designs like single channel serpentine force water out of the system and prevent flooding which allows them to operate better at high power, but at low power draw they may dry out the membrane unless humidified gasses are supplied. Supplying humidified gasses increases the cost and complexity of a fuel cell system. Transportation applications require fuel cells to operate at both low and high power demands and at various relative humidity values so the design should perform equally well across a wide range of operating conditions.

Overall conductivity of the cell, as well as contact resistance between the gas diffusion layer (GDL) and the bipolar plate, is greatly influenced by the flow field design. Low conductivity (high resistance) creates ohmic losses in the cell that reduce the performance. Fig. (**1**) shows that the flow field is an electronically insulating void carved into the conductive bipolar plate. The bipolar plate has a much higher

*Address correspondence to this author at the Fuel Cell Laboratory, Department of Engineering and Computing Systems, Arizona State University, Mesa, AZ 85212, USA, E.mail: amk@asu.edu

conductivity than the GDL so the path from the reaction site to the bipolar plate should be as short as possible in order to minimize ohmic losses. This means that flow field channels should be made narrow; however, narrowing the channels also increases their resistance to gas flow. In addition, extremely narrow channels with corresponding narrow land areas may reduce the durability of the cell and can pose a challenge during manufacturing. The bipolar plate also provides physical support for the membrane electrode assembly (MEA). Overly wide channels not only reduce conductivity, but can also allow the MEA to deform under clamping pressure or gas pressure.
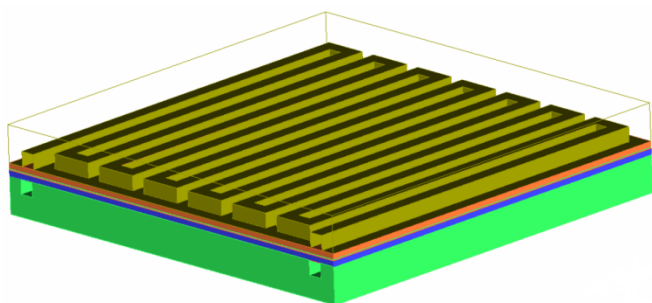

Fig. (1). Schematic ofa 5 cm^2 serpentine fuel cell assembly with anode flow plate made transparent to reveal the channel geometry.

The final important role of the flow field is to minimize friction to gas flow. This is generally measured using the gas pressure drop from inlet to outlet. Designs that have long paths from inlet to outlet will have more friction and require external blowers to force gas through the system. Increasing the operating pressure inside the cell does have a positive influence on the reaction rate, but these additional components impose a parasitic load and add to the cost, weight and complexity of a fuel cell system.

The flow field has several important roles to play in high PEMFC performance. One way to improve flow field geometry is to consider designs inspired by natural phenomena. These can include biological fluid or gas delivery systems, in addition to other systems found in the natural world that often display fractal features. Our recent review describes a number of nature inspired designs [2] ranging from strictly mathematically-based fractal designs to non-formal heuristic designs which draw on inspiration from leaves and lungs. Other recent reviews of flow field designs have focused more on the effects of varying specific geometrical parameters such as channel height and shape [3].

One of the most important optimization parameters for a flow field is pressure drop. A low pressure drop reduces the energy required to pump fuel through the system thus increasing overall system efficiency. Unfortunately, low pressure drop will often create issues with flooding at high current densities because water will be allowed to pool in the flow channels instead of being forced out by gas pressure. Experimental studies by Spernjak have shown that interdigitated designs offer a middle ground between high performance, high pressure serpentine designs and low pressure, flooding prone parallel designs [4]. Our aim is to improve interdigitated designs by applying biologically inspired branching rules. These rules create more mathematically formal descriptions of flow field designs which can be optimized more easily. We use numerical simulations to evaluate a number of candidate designs against standard designs for pressure drop, current density, and current distribution.

2. MODELING AND SIMULATION OF A PEMFC

A commercialthree dimensional computational fluid dynamics (CFD) fuel cell simulation software package was used to evaluate several standard and novel fuel cell flow field designs. All simulations were carried out using Ansys Fluent version 13.0 with the fuel cell module add-on. Computational meshes were created by Ansys ICEMCFD version 14.0 using a Cartesian grid method. Modeling parameters and boundary conditions which were common across all simulations are listed in Table **1**. Details of the mathematical model can be found in the appendix of our previous publication [5].

Table 1. Model parameters used in the PEMFC performance simulation.

No.	Parameter	Value
1	**Flow field plate**	
	Density	1.99 g cm^{-3}
	Specific heat capacity	710 J kg^{-1} K^{-1}
	Thermal conductivity	120 W m^{-1} K^{-1}
	Electrical conductivity	926 S cm^{-1}
	Thickness	2.5 mm
2	**Gas diffusion layer**	
	Density	0.321 g cm^{-3}
	Porosity	82%
	Electrical conductivity	2.8 S cm^{-1}
	Wetting angle	110 degrees
	Thickness	300 μm
3	**Catalyst layer**	
	Surface-to-volume ratio	1.25 x10^7 m^2 m^{-3}
	Anode and cathode thickness	6 and 12 μm
4	**Electrolyte (Nafion-212)**	
	Thermal conductivity	0.16 W m^{-1} K^{-1}
	Ionic conductivity	0.1 S cm^{-1}

A mesh sensitivity analysis was performed on a single design to determine the required maximum mesh cell size which produced grid-independent results. Final mesh sizes for our 5 cm^2 geometry ranged from 500,000 to 750,000 elements. The number of vertical divisions in the MEA was kept constant at 5 divisions in the GDL and catalyst layers

and 10 divisions in the membrane. Our preliminary investigations found that increasing the number of vertical divisions in these parts did not affect the predicted polarization curves.

Convergence criteria were established based on techniques described in Arvay *et al.* [5]. Current convergence, as well as hydrogen and oxygen species convergence, were monitored and the simulation was considered convergent when the following three conditions were satisfied: The reported current at the cathode terminal changed by less than 0.5% or less (over 5,000 iterations); the hydrogen species consumption matched the reported current within 25%; and the reported oxygen species consumption matched the reported current within 1%. Species consumption error is calculated by comparing the reported current at the terminals to the expected current generated by the consumed species. In general these convergence criteria were satisfied after approximately 6,000 iterations which took approximately 20 hours using a 2.6 GHz Intel Xeon based quad-core system. Fig. (**2**) shows examples of the convergence behavior of a select data points for one simulation. The behavior asymptotically approaches a finalized value demonstrating that the reported solution would not change with additional computational time. The purpose of using these three convergence criteria rather than monitoring residual alone was to ensure that the physically measurable experimental values were all approaching a constant value.
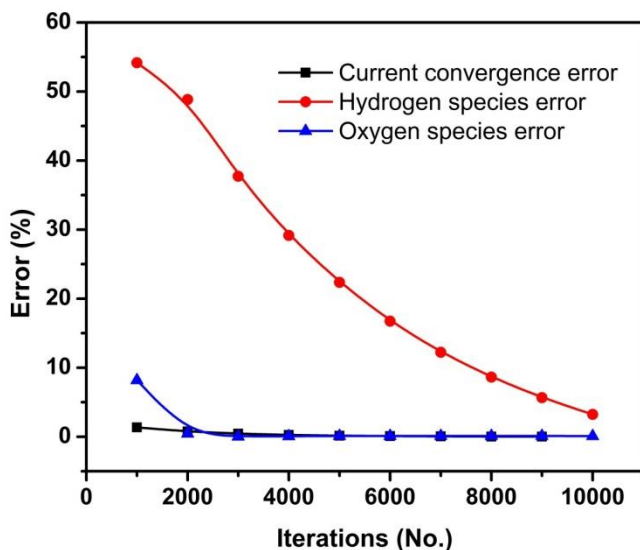

Fig. (2). Convergence behavior of a select data point. It shows that the errors are trending towards zero with the increasing number of iterations,which suggests that the solution is converged.

The MEA, consisting of the membrane, anode and cathode catalyst layers and anode and cathode GDLs, was kept identical in all the simulations and only the flow field design was varied between simulations. The MEA was modeled after an experimental cell with an active area of $5 cm^2$. Measurements of the flow channel dimensions andGDL thicknesswere taken. All other physical parameters used in the model were adopted from previous studies and areshown in Table **1** [5, 6] Five steady-state, isothermal, potentiostatic data points were collected for each simulation

at 0.9, 0.8, 0.7, 0.5 and 0.3 volts. Data collection was stopped at 0.3 V because that voltage value is generally close to peak power output and going beyond peak power is not useful for our study. Potentiostiatc boundary conditions were chosen rather than galvanostatic because the maximum and minimum voltage values are known in advance. The data was collected in descending order and the final value of the previous data point was used as the initial condition for the next data point.

A single channel serpentine test cell was used for experimental verification of model parameters. Open circuit voltage of the experimental cell was measured to be 0.98 V. Simulated and experimental polarization curves show good agreement as seen in Fig. (**3**). The contact resistance was adjusted and a final value of 1.0×10^{-6} ohm·m^{-2} was used for all designs. This value is known to vary depending on the clamping pressure of the cell but for the purposes of these simulations it was assumed to remain constant between each design. The channel to land ratio for each design was also kept close to 1.0 in order to minimize variation due to contact resistance between each design.
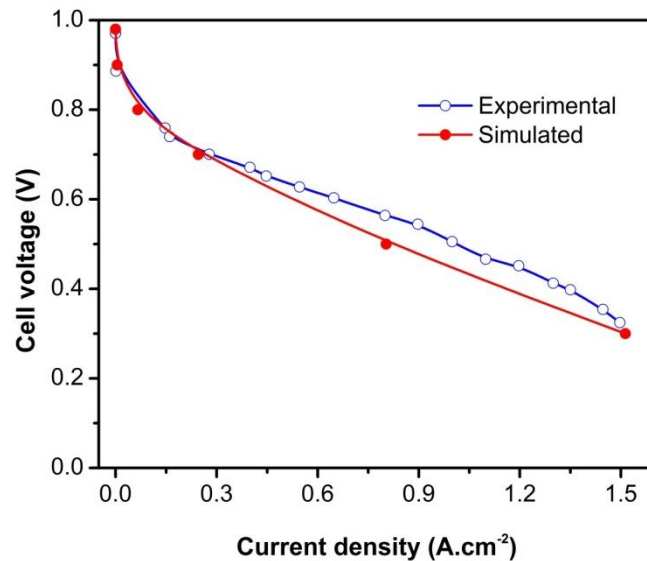

Fig. (3). The polarization curves of the standard serpentine design from both experimental and simulated studies. The good agreement between experimental and simulated data provides verification of our simulation models.

CFD modeling is a useful tool for investigating PEMFC performance but several important limitations need to be recognized. CFD models of PEMFCs generally have difficulty making accurate predictions of liquid water formation and transport. Liquid water that is formed in this model implementation is assumed to be contained in fine water droplets which move with the gas stream. This means that the accuracy of this model is questionable at high current densities when flooding is likely to occur. Available computational resources also necessitate that our simulations be run at steady state rather than transient, so behavior over time is not predicted. Despite these limitations, CFD modeling is a useful tool for comparing the uniformity of gas distribution and pressure drop of a particular flow field

design. Experimental studies are necessary to investigate the water transport characteristics of a cell.

3. FLOW FIELD DESIGNS

Simulations by Kloess *et al.* showed that performance of interdigitated designs inspired by lungs and leaves is higher than traditional interdigitated designs [7]. Experimental studies of a 25 cm^2 cell by Spernjak *et al.* showed that interdigitated designs have good water management characteristics with reduced pressure drop compared to serpentine designs [4]. Numerical and experimental studies by Currie [8] showed that a design which followed Murray's branching law (Eq. 1) offered more uniform gas distribution compared to a standard parallel design. However, experimental results on parallel designs from Spernjak *et al.* [4] and Currie [8] both show that parallel designs have poor water management characteristics and are more likely to flood than other designs, which reduces the performance of parallel designs. We combined these design principles in order to create several interdigitated designs for a 5 cm^2 cell which follows the branching law. Standard designs were also simulated for comparison.

Murray's branching law states that the cube of the radius of the parent branch should be equal to the sum of the cubes of the radii of the daughter branches.

$$r_p^3 = r_{d1}^3 + r_{d2}^3 + \cdots + r_{dn}^3 \qquad (1)$$

where r$_p$ is the radius of the parent channel and r$_d$ are the radii of the daughter channels. This simple relation has been found to hold true in the pulmonary and vascular systems of animals as well as in the non-load-bearing xylem of plants [9]. Our implementation of this rule for PEMFC flow fields replaces the radius of a round channel with the length of a side of a square channel.

One limitation of implementing this constraint in flow field designs is the minimum and maximum width of the flow field channel. Channels that are too narrow make manufacturing difficult; however, a channel that is too wide would have electron conductivity issues. Obeying the branching relation and having *n* daughter channels with equal dimension causes daughter channels to be $\frac{1}{\sqrt[3]{n}}$ times smaller than the parent. A node that splits into 3 channels (n=3) means that each daughter channel is $\frac{1}{\sqrt[3]{3}}$ or 0.7 times smaller than that of the parent. A second branch node would create the daughter channels 0.7 times smaller again, which means the smallest channel would be half the size of the largest channel with two branch nodes. Therefore, the number of branch nodes along a given path must be limited to 3 or less in order to maintain reasonable channel dimensions.

A total of 11 designs, shown in Figs. (**4** and **5**), were simulated using the fuel cell model. Three different traditional flow field patterns were simulated for reference. A standard serpentine design was created based on the experimental test cell and used for simulation validation. The standard serpentine design measurements were used as the basis for creating standard parallel and standard interdigitated geometry. The standard designs served as a performance benchmark to evaluate novel interdigitated
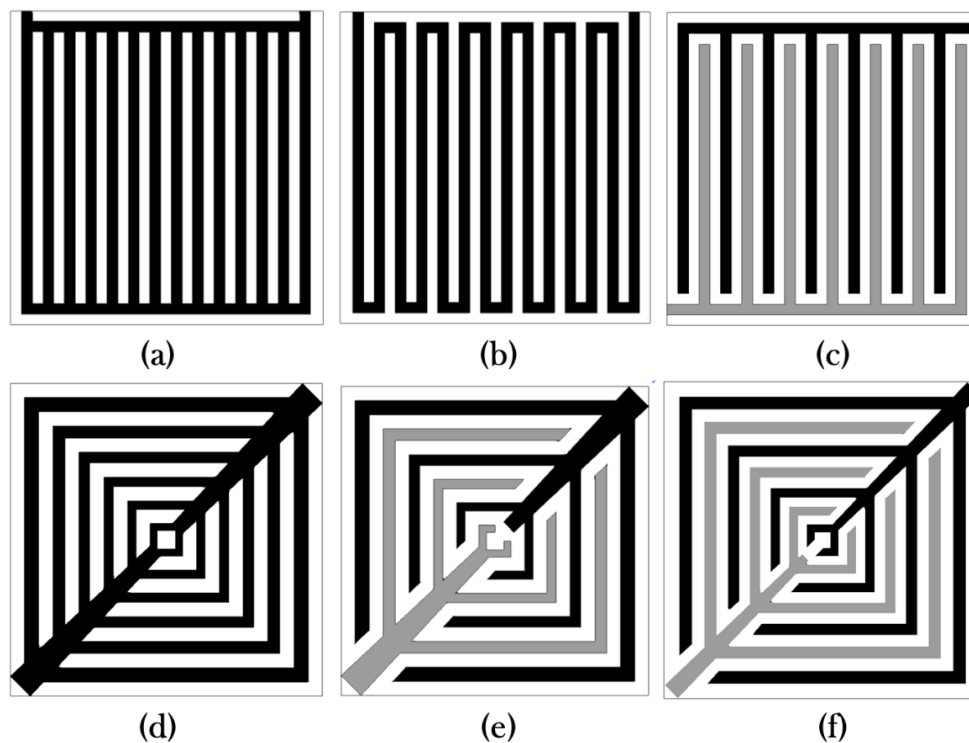

Fig. (4). Schematic representation of flow field designs: (**a**) Standard parallel, (**b**) Standard serpentine, (**c**) Standard interdigitated, (**d**) Murray-parallel, (**e**) Murray-interdigitated-1 and (**f**) Murray-interdigitated-2. The inlet channels are shaded gray and the outlet channels are black.

designs.

The standard designs (Figs (**4a-4c**)) have the same individual channel dimensions of 0.8 mm tall by 0.8 mm wide.Land widths were made equal to channel widths. The Murray-parallel design (Fig. (**4d**)) has channels with a constant depth of 0.8 mm while channel widths vary according to Murray's law. An interdigitated design was created from the Murray-parallel design (Fig. (**4e**)) by adding baffles at the end of every other channel pair. The land widths remained constant in the Murray-interdigitated-1 design. Inspection of the current density contours led to a revision of this design (Fig. (**4f**)). The revised design started with a narrower inlet channel and set land width to same width as the adjacent channel instead of being constant. Performance of the revised design was inferior to the standard interdigitated design so no further revisions were made.

Close examination of the current density performance of the standard interdigitated design showed that current density values were lower further from the inlet. This observation led to a centered inlet pitchfork design which created more uniform distance from the inlet to the end of each channel. Five interdigitated designs based on a pitchfork pattern were created and evaluated in sequence (Figs. (**5a-5e**)) with each design attempting to improve on the performance of the previous design.

The Pitchfork-7 designs have a total of 7 inlet channels. The channel dimensions obey Murray's branching law with aspect ratios set square so that channel heights as well as widths vary within the design. Adjacent land widths were set equal to the channel width in order to maintain a channel to land ratio close to 1.0. Table **2** shows the channel to land ratios of the final designs. The channel widths were constrained to a width of 0.6 mm or greater for manufacturing simplicity and a maximum channel width of 1.4 mm was imposed to maintain electronic conductivity of the design. Designs were varied by changing the channel lengths and the number of daughter channels created at a branch. The outlet channels were given the same dimensions as corresponding inlet channels. This means that the outlet channels do not strictly adhere to the branching law. The pressure gradient in the outlet channel of an interdigitated design is very small compared to the inlet, so optimizing pressure drop for the outlet channel is not as vital.

Experimental measurements have shown that contact resistance can vary significantly with flow field design and compression, but this value was assumed invariant between designs in order to simplify the comparison. Gas flow is fed in a counter flow pattern where hydrogen and air enter the cell at opposite ends. Flow rateswere set at constant rates of 1.74×10^{-7} kg·s^{-1}of 100% RH hydrogen at the anode and 5.4×10^{-6} kg·s^{-1}of 100% RH air at the cathode. These values correspond to a stoich of approximately 2 at the maximum current density of 1.5 A·cm^{-2}. This stoich value is lower than typical experimental values of about 3 for air flow but is consistent between all simulations in our study.
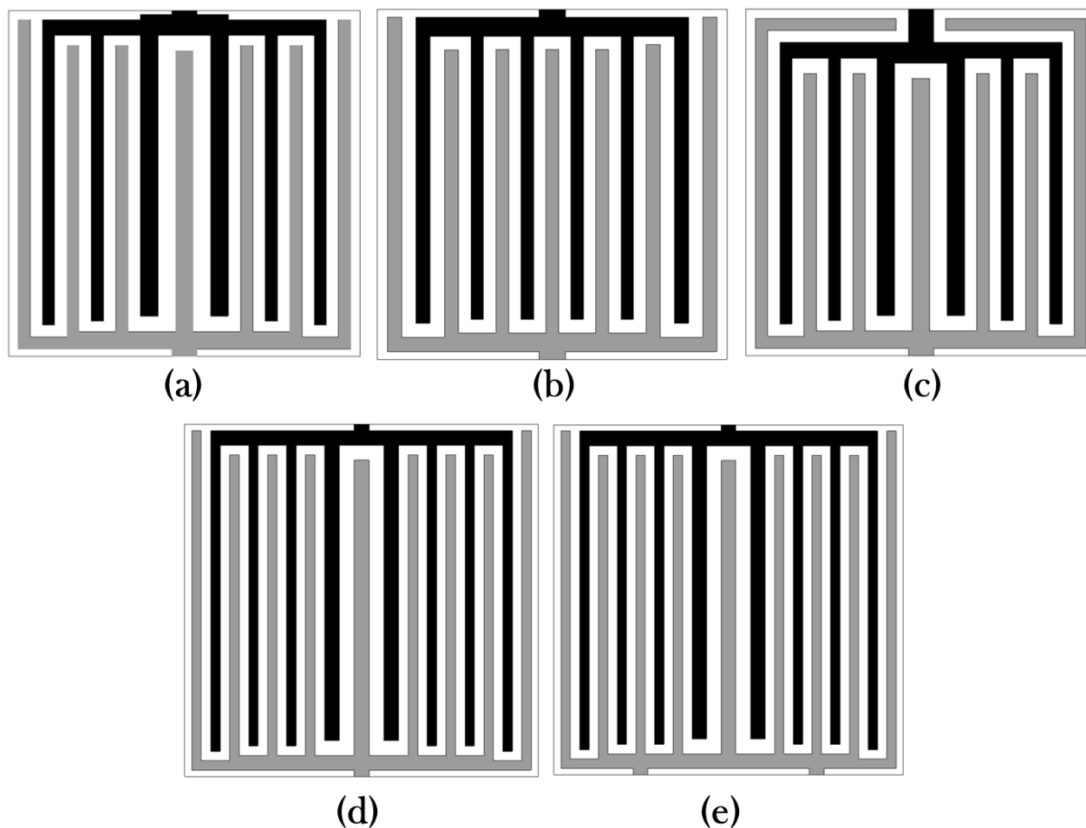

Fig. (5). Schematic representation of various biologically inspired flow field designs: (**a**) Pitchfork-7a, (**b**) Pitchfork-7b, (**c**) Pitchfork-7c, (**d**) Pitchfork-9a and (**e**)Pitchfork-9b. The inlet channels are shaded gray and the outlet channels are black.

4. RESULTS AND DISCUSSION

Fig. (**6**) shows the polarization data from all of the designs using hydrogen and air at 100 % RH. The standard serpentine design offers the highest current density performance while the standard parallel design has the lowest performance. The Murray-parallel design offers greatly improved performance over a standard parallel design. This is consistent with previous studies of biologically inspired parallel designs. Polarization data show that all the designs perform similarly at low current density and show more divergence at higher current density values. The highest performance design at this size scale is the standard serpentine design.

Current density distributions at the cathode catalyst layer at 0.3 V are shown in Fig. (**7**). Examining current density contours can offer some insight into the cause of differences in performance among various designs. Ideal contours will show little variation between different areas of the cell. Visual inspection suggests that the standard serpentine and Pitchfork designs offer the most uniform current distribution. The Murray-parallel and Murray-interdigitated contoursin Figs (**7d-7f**) all show non-uniform current density distributions with large patches of red indicating high activity towards the edges of the cell and areas of blue indicating low activity towards the center of the cell.

Quantitative measures of these differences are calculated

Table 2. **Simulation performance data for various bioinspired flow field designs along with the standard parallel and serpentine patterns.**

| Designs	Channel/Land Ratio	Anode Pressure Drop (Pa)	Cathode Pressure Drop (Pa)	Current Density at 0.3V (A.cm^{-2})	Current Density Deviation (%)
Standard parallel	0.95	4	212	0.92	66
Standard serpentine	0.89	175	3295	1.50	37
Standard interdigitated	0.88	131	5688	1.41	47
Murray-parallel	0.87	2	36	1.40	56
Murray-interdigitated-1	0.79	225	9598	1.38	58
Murray-interdigitated-2	0.83	200	6655	1.30	65
Pitchfork-7a	1.01	155	6328	1.46	42
Pitchfork-7b	1.00	162	6351	1.41	42
Pitchfork-7c	1.00	154	6400	1.46	44
Pitchfork-9a	0.98	101	4155	1.46	42
Pitchfork-9b	1.02	102	4127	1.45	44
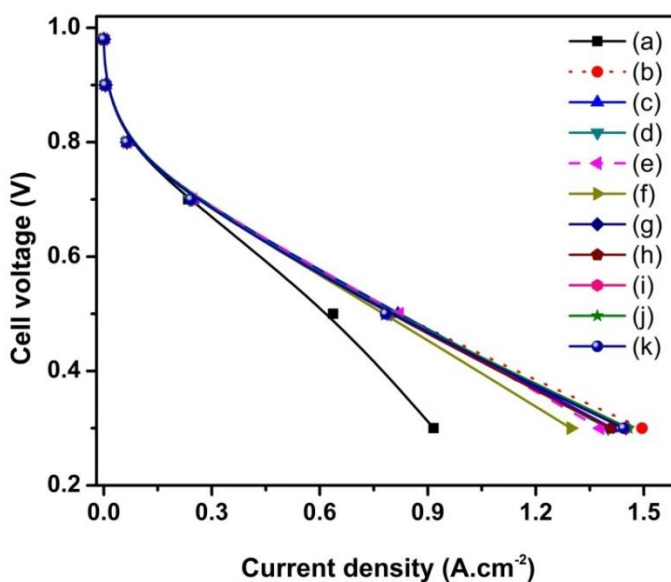
Fig. (6). Polarization data for (**a**) Standard parallel, (**b**) Standard serpentine, (**c**) Standard interdigitated, (**d**) Murray-parallel, (**e**) Murray-interdigitated-1, (**f**) Murray-interdigitated-2, (**g**) Pitchfork-7a, (**h**) Pitchfork-7b, (**i**) Pitchfork-7c, (**j**) Pitchfork-9a and (**k**) Pitchfork-9b.
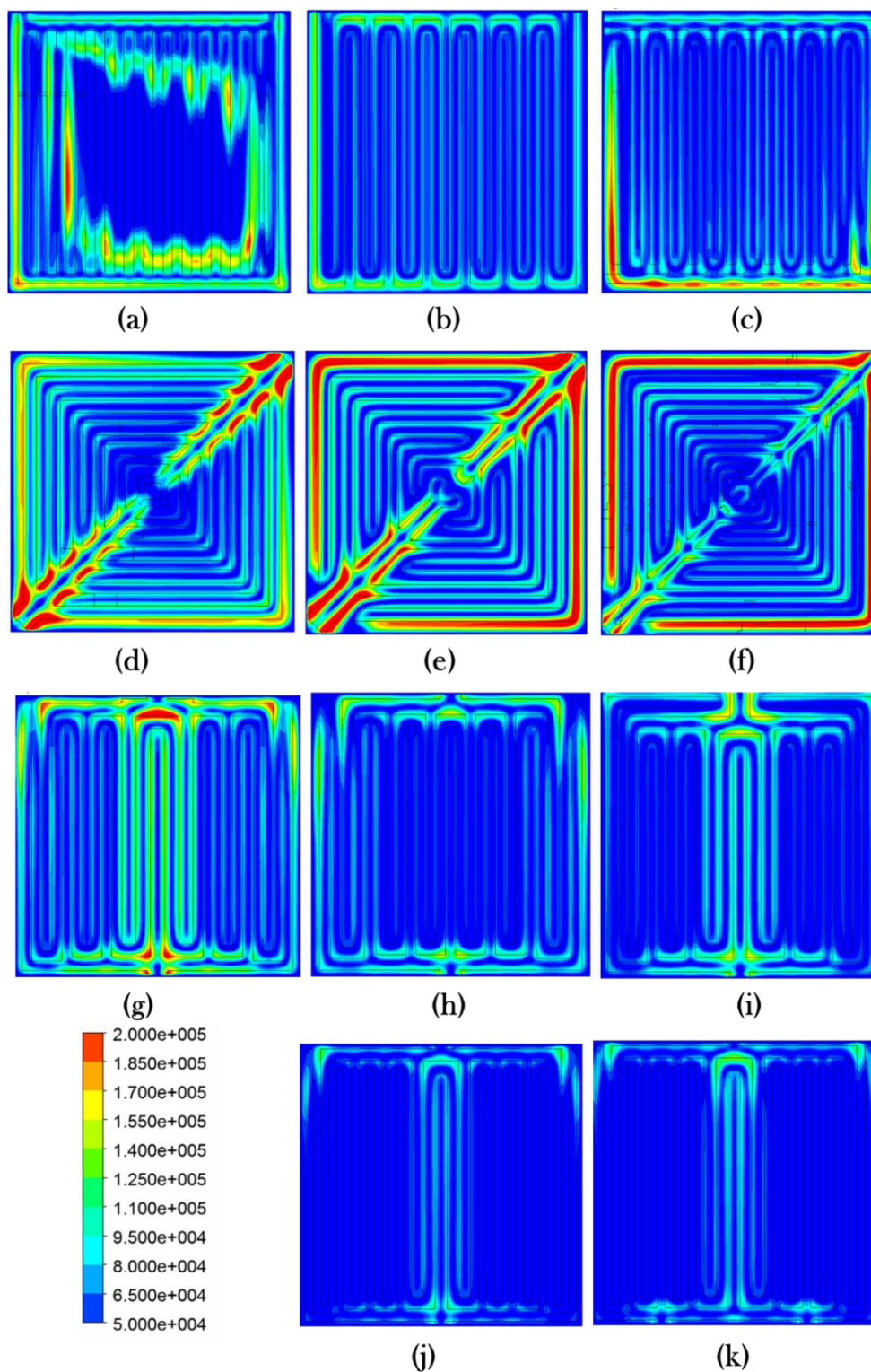
Fig. (7). Current density contours for (**a**) Standard parallel, (**b**) Standard serpentine, (**c**) Standard interdigitated, (**d**) Murray-parallel, (**e**) Murray-interdigitated-1, (**f**) Murray-interdigitated-2, (**g**) Pitchfork-7a, (**h**) Pitchfork-7b, (**i**) Pitchfork-7c, (**j**) Pitchfork-9a and (**k**) Pitchfork-9b. Lower limit set above zero to better highlight areas of excessively high current density.

using percent current density deviation as shown in table 2. The percent current density deviation is calculated by dividing the standard deviation of current density by the mean current density. This measure is a way of quantifiably expressing the variation seen in the contour maps so it can be directly compared across designs. A low coefficient of variation means that the current is more uniform across the active area.

w Table **2** also summarizes other performance characteristics of each design. The channel to land ratio was calculated by simply dividing the total channel area by the total land area. Anode and cathode pressure drops were measured in Pascals at the respective inlet and outlet surfaces. Reducing pressure drop is one method of improving performance by reducing the parasitic load of external blowers. Current density at 0.3 V represents the highest current density value measured in the simulation data at the terminals. Polarization data show that flow field design plays a more critical role at higher current densities.

Pressure drops across the anode side were relatively low compared to that of the cathode side due to much lower flow rates of hydrogen gas, lower density, and higher diffusivity rates compared to that of air in the anode side. Cathode side pressure drop was lowest for parallel designs. Increasing the total number of channels (inlet plus outlet) in an interdigitated design generally reduced overall pressure drop. The Murray-interdigitated-1 (Fig. **4e**) design had a total of 12 channels, the Murray-interdigitated-2 (Fig. **4f**) and standard interdigitated (Fig. **4c**) design had a total of 14 channels, the Pitchfork-7 designs had 15 channels, and the Pitchfork-9 designs had 17 channels. Pressure drop values suggest that different branching schemes with the same number of total channels have little effect on the overall pressure drop. Pressure drops on the anode side of the Murray-parallel designs were much lower than the standard parallel designin agreement with the findings in the original study [8]. Anode side pressure drop of the standard interdigitated design was lower than that of the Murray-interdigitated designs which suggests that the Murray-interdigitated design can be improved. The data in Table **2** show that the Pitchfork-7a,-7b and -7c designs show improved current density variation over the standard interdigitated design while maintaining equivalent current density performance. The current density contour for the first Pitchfork design shows an area of higher current density around the center channel (Fig. **7g**). The design was altered by narrowing the center channel and increasing the size of the outer channels leading to the Pitchfork-7b design. Current density contours for this new design (Fig. **7h**) show that the area of higher current density around the center channel is removed; however, the overall performance of the cell was reduced. The cathode pressure drop of these two designs was still higher than the standard interdigitated design. A third design was developed in an attempt to recover the performance of the original Pitchfork design and reduce the pressure drop. This design increased the channel length of the outer most channels creating a wrapped design. It was hoped that this would reduce the pressure drop by creating a larger flow path to the outlet channels. The current density contour in Fig. (**7i**) shows a similar pattern as Fig. (**7g**) but data from table 2shows that pressure drop did not decrease and current uniformity became worse. It is likely that the longer channel lengths offset any gains from additional under-land flow path. The pitchfork design principle was further altered in an attempt to optimize the current density distribution and reduce pressure drop by increasing the under-land flow path without increasing channel lengths.

The original Pitchfork 7 design was modified to a 9-branch design. All channel dimensions were made slightly narrower to accommodate the increased number of channels. The new design maintained the same current density performance and variation characteristics while reducing the pressure drop. It can be seen from the contours (Fig. (**7j** and **7k**)) that the center channel of the Pitchfork-9 designs still has a noticeably higher current density values than the rest of the channels, but not as drastic asthe Pitchfork-7a design. The first 9-channel pitchfork design was modified by splitting the inlet into two separate inlets (Fig. (**7k**)) with equivalent overall massflow. It was thought that the higher current density values were being caused by being closer to the inlet gasses. Results from this revision showed virtually no performance improvement which suggests that the position of the inlets is not critical.

The current density distribution was improved and the pressure drop was reduced in the Pitchfork-9a optimized design compared to all other interdigitated designs. This is a promising result which merits further investigation. As noted before these simulations are limited by the inability to predict liquid water and the standard serpentine design still offers the best performance overall at this size scale. The experimental study by Spernjak [4] showed that interdigitated designs have lower pressure drops than single serpentine at 25 cm^2 size scales. This suggests that interdigitated designs scale up more efficiently than single serpentine which merits further investigation for biologically inspired interdigitated designs in larger cells.

CONCLUSION

PEMFC flow field design plays a critical role in fuel cell performance. Complex designs are difficult to describe using formal mathematics which makes it challenging to optimize these designs in a systematic way. The use of biologically inspired designs which follow Murray's branching law is one approach which can formalize some aspects of design creation. Physical and manufacturing constraints can be included as part of the design optimization. In these simulation studies, interdigitated designs using a Pitchfork pattern and following Murray's branching law have more uniform current density distributions but increased pressure drops, for the same overall number of channels. We found that different branching patterns with the same number of total branches have little effect on pressure drop but will change the current density distribution. Increasing the under-land convection area will decrease pressure drop as long as channel lengths are not increased as well. Additional research is needed to verify performance of these novel designs in experimental cells where flooding can be observed and at larger size scales where previous studies have indicated more drastic performance differences between interdigitated and serpentine patterns.

CONFLICT OF INTEREST

The author confirms that this article content has no conflict of interest.

REFERENCES

[1]   Ahluwalia, R.K.; Wang, X. Fuel cell systems for transportation: status and trends. *J. Power Sources,* **2008**, *177*, 167-176.

[2]   Arvay, A.; French, J.; Wang, J.C.; Peng, X. H.; Kannan, A. M. Nature inspired flow field designs for proton exchange membrane fuel cell – Review. *Int. J. Hydrogen Energ.,* **2013**, *38*, 3717-3726.

[3]   Manso, A.P.; Marzo, F.F.; Barranco, J.; Garikan, X.; Mujika, G. Influence of geometric parameters of the flow fields on the performance of a PEM fuel cell. A review. *Int. J. Hydrogen Energ.*, **2012**, *37*, 15256-15287.

[4]   Spernjak, D.; Prasad, A.K.; Advani, S.G. *In situ* comparison of water content and dynamics in parallel, single-serpentine, and interdigitated flow fields of polymer electrolyte membrane fuel cells. *J. Power Sources,* **2010**, *195*(11), 3553-3568.

[5]   Arvay, A.; Ahmed, A.; Peng, X.H.; Kannan, A.M. Convergence criteria establishment for 3D simulation of proton exchange membrane fuel cell. *Int. J. Hydrogen Energ.*, **2012**, *37*, 2482-2489.

[6]   Iranzo, A.; Munoz, M.; Rosa, F.; Pino, J. Numerical model for the performance prediction of a PEM fuel cell. Model results and experimental validation. *Int. J. Hydrogen Energ.*, **2010**, *35*, 11533-11550.

[7]   Kloess, J.P.; Wang, X.; Liu, J.; Shi, Z.; Guessous, L. Investigation of bio-inspired flow channel designs for bipolar plates in proton exchange membrane fuel cells. *J. Power Source,* **2009**; *188*, 132-140.

[8]   Currie, J.M. *Biomimetic Design Applied to the Redesign of a PEM Fuel Cell Flow Field.* Mechanical and Industrial Engineering, University of Toronto, Ottawa, **2010**.

[9]   Sherman, T.F. On connecting large vessels to small. The meaning of Murray's law. *J. Gen. Physiol.*, **1981**, *78*, 431-453.